Structural Engineering and Mechanics, *Vol. 73, No. 5 (2020) 515-527*
DOI: https://doi.org/10.12989/sem.2020.73.5.515

A stress field approach for the shear capacity of RC beams with stirrups

Dario De Domenico*[1] and Giuseppe Ricciardi[1]

Department of Engineering, University of Messina, Contrada Di Dio, Villaggio Sant'Agata, 98166 Messina, Italy

(Received June 22, 2019, Revised October 16, 2019, Accepted October 19, 2019)

Abstract. This paper presents a stress field approach for the shear capacity of stirrup-reinforced concrete beams that explicitly incorporates the contribution of principal tensile stresses in concrete. This formulation represents an extension of the variable strut inclination method adopted in the Eurocode 2. In this model, the stress fields in web concrete consist of principal compressive stresses inclined at an angle $\boldsymbol{\theta}$ combined with principal tensile stresses oriented along a direction orthogonal to the former (the latter being typically neglected in other formulations). Three different failure mechanisms are identified, from which the strut inclination angle and the corresponding shear strength are determined through equilibrium principles and the static theorem of limit analysis, similar to the EC-2 approach. It is demonstrated that incorporating the contribution of principal tensile stresses of concrete slightly increases the ultimate inclination angle of the compression struts as well as the shear capacity of reinforced concrete beams. The proposed stress field approach improves the prediction of the shear strength in comparison with the Eurocode 2 model, in terms of both accuracy (mean) and precision (CoV), as demonstrated by a broad comparison with more than 200 published experimental results from the literature.

Keywords: reinforced concrete beam; limit analysis; shear strength; principal tensile stresses; smeared truss model; concrete compression struts; transverse reinforcement; Eurocode 2; stirrups; variable strut inclination method

1. Introduction

The determination of the shear capacity of reinforced concrete (RC) members is a critical research subject that has attracted the attention of many investigators in the last few decades (Regan 1969, Park and Paulay 1975, Wang *et al*. 2005, Londhe 2009). A RC element is typically subjected to combined shear and flexure, which triggers complex multi-axial stress states. The shear failure is typically associated with diagonal cracks and is generally more brittle than flexural failure (Russo and Puleri 1997, Keskin 2017, Qissab and Salman 2018). The presence of transverse reinforcement, commonly represented by vertical stirrups, attenuates brittle phenomena and contributes to increasing the shear capacity (Collins *et al*. 2008, Park *et al*. 2015).

The simplest approach to predict the shear strength of RC members with transverse reinforcement is based on the truss analogy and simple equilibrium conditions. Ritter (1899) and Mörsch (1908) proposed a very simple strut-and-tie model at the beginning of the past century, formed by parallel chords and web members. The parallel chords describe the concrete stress blocks and longitudinal reinforcement. The web members incorporate the shear transfer actions of inclined compressive struts and tensile ties. The struts represent concrete stress fields between adjacent cracks, and are inclined at an angle θ with respect to the beam longitudinal axis, while the tensile ties represent the transverse reinforcement or stirrups. In the Ritter-Mörsch (RM) model the strut inclination angle is given a particular value, namely $\theta = 45°$, which coincides with the first shear cracking angle. Experimental investigations (Leonhardt 1973) demonstrated that this was a very conservative assumption and that this model largely underestimated the actual shear strength of RC beams. It is widely accepted that besides the truss action, included in the RM model, many other shear transfer mechanisms take place while the level of load increases, such as aggregate interlock, residual tensile stresses, shear stresses carried by the un-cracked compression chord, and dowel action (ACI 445R-99, Russo *et al*. 2013). Based on these mechanical considerations, many theories and rational approaches were proposed to modify or improve the RM model, based on similar truss models (Li and Tran 2012, He *et al*. 2015, Yavuz 2016). Some well-established theories, such as the modified compressive field theory (MCFT) or other compatibility-aided theories (Vecchio and Collins 1986, Hsu 1988), used compatibility conditions in addition to equilibrium principles to determine the shear capacity. Despite their proven accuracy, these theories generally imply specialized knowledge and computer programs for their application, which is not convenient in daily engineering practice. However, these compatibility-based considerations inspired design formulations implemented in building codes in a simplified manner.

Some models preserved the assumption $\theta = 45°$ for the strut inclination angle, but included an explicit concrete contribution as a correction term of the RM model (additive approach), such as the ACI 318 code (ACI, 2011) and the European pre-standard ENV 1992-1-1. On the other hand, the Model Code 2010 (fib 2013) incorporated different levels of approximation for the calculation of the shear

*Corresponding author, Ph.D.
E-mail: dario.dedomenico@unime.it

http://www.techno-press.com/journals/sem&subpage=7
ISSN: 1225-4568 (Print), 1598-6217 (Online)

capacity of RC members with transverse reinforcement, in which the most precise method implies an additive approach where a concrete contribution is added explicitly (based on a simplified version of the MCFT), while the simplest approach neglects the concrete contribution and considers strut inclination angles θ less than 45° (Sigrist *et al*. 2013). Strut rotations at ultimate limit state lower than the first shear cracking angle were observed experimentally (Walraven *et al*. 2013) and depend upon amount of transverse reinforcement, concrete strength and beam cross-section characteristics. Some other models, such as the Model Code 90 (fib 1993), the Eurocode 2 (EC2) (EC2 2005) as well as national building codes in European countries, such as Italian (NTC 2018) and German codes (DIN 1045-1 2008), used a general variant of the RM model (without explicit concrete contribution) in which variations of the strut inclination angle θ are allowed within a certain range (variable strut inclination method). In these models, the determination of the ultimate strut inclination angle θ_u is carried out in the framework of the lower-bound theorem of plasticity, or static theorem of limit analysis (Back *et al*. 1978, Nielsen and Hoang 1999). In particular, the angle θ_u maximizes the shear strength within the class of statically and plastically admissible solutions, i.e., the class of solutions satisfying equilibrium conditions and nowhere violating yield conditions. This design philosophy is similar to the stress field approach (Sigrist 2011), which combines limit analysis with a continuous representation of the web of the beam as a composition of membrane elements subjected to in-plane stresses, the cracked membrane model (Kaufmann and Marti 1998). In a wider context, many researchers demonstrated the effectiveness of limit analysis procedures to predict the ultimate capacity of RC members (Limam *et al*. 2003a, 2013b, Le *et al*. 2010, 2017, Spiliopoulos and Weichert 2014, Fuschi *et al*. 2015, De Domenico *et al*. 2014, 2018, Pisano *et al*. 2013, 2015).

Along this research line, this paper presents a stress field limit analysis approach based on the concept of cracked membrane element in combination with the variable strut inclination method of the Eurocode 2. As a distinctive peculiarity of the proposed approach, in addition to the principal compressive stresses, also the contribution of the principal tensile stresses in the cracked membrane is explicitly included in the shear strength calculation procedure. This is a novelty in comparison to the EC-2 approach as well as to other formulations proposed in the literature. It is reasonable to think that concrete membrane between two adjacent cracks is subject to a biaxial stress state formed by principal compressive and tensile stresses, where the latter are oriented along a direction orthogonal to the former. In line with the EC-2 approach, the expressions governing the shear capacity of a RC beam are derived based on equilibrium conditions, while the ultimate strut inclination angle θ_u is determined in the framework of the lower-bound theorem of plasticity. Including the principal tensile stresses slightly increases the strut inclination angle θ_u and significantly improves the prediction of the shear strength with respect to the EC-2 approach, as demonstrated by a comparison with more than 200 experimental results from the literature.

2. Stress field approach and shear strength calculation

The concept of cracked membrane model was developed many years ago (Kaufmann and Marti 1998) and is schematically represented in Fig. 1. The segment of an RC beam is split into a tension and a compression chord and the web. In the web, the cracked membrane can be assumed to undergo a plane stress condition state. In particular, the membrane element is generally subjected to in-plane stresses $\sigma_x, \sigma_z, \tau_{xz}$. The corresponding principal compressive and tensile stresses $\sigma_{ccw}, \sigma_{ctw}$ are oriented along the directions θ and $\pi/2-\theta$ with respect to the beam longitudinal axis, respectively. Concurrently, the membrane element is also subjected to tensile stresses due to the transverse reinforcement (i.e., the cracked membrane is orthogonally reinforced). The spacing of stirrups is assumed small enough so that their actions can be modeled with uniform stress fields σ_{sw}, according to the smeared truss model concept (Marti 1985).

In order to evaluate the shear capacity of the RC beam in the proposed stress field approach, it is sufficient to impose equilibrium conditions on different beam segments that are determined through different sections on the continuous model in Fig. 1. In particular, three different sections are studied, which correspond to three different failure mechanisms of the RC beam. The first failure mechanism is identified by the vertical equilibrium across the first beam segment obtained through a section parallel to the compression struts θ, cf. the sketch of Fig. 2. The stress fields contributing to this failure mechanism are the tensile stresses of stirrups and the principal tensile stresses of concrete. Typically, the inner lever arm z can be assumed as $0.9d$, in which d represents the effective depth of the beam cross-section. The number of stirrups crossing the beam segment $\overline{AD}$ is computed under the hypothesis of a constant spacing s, which leads to

$$n_{s1} = \frac{\overline{AD}}{s} = \frac{z(\cot\theta + \cot\alpha)}{s} \tag{1}$$

As said above, assuming a uniform stress field of stirrups equal to σ_{sw}, and denoting with A_{sw} the area of the corresponding cross-section, the resultant tensile force of the transverse reinforcement is given by

$$S_{s1} = \sigma_{sw} A_{sw} n_{s1} = \sigma_{sw} A_{sw} \frac{z(\cot\theta + \cot\alpha)}{s} \tag{2}$$

On the other hand, the contribution of principal tensile stresses of concrete to this failure mechanism can be computed as follows

$$S_{ct1} = \sigma_{ctw} b_w \overline{AB} = \sigma_{ctw} b_w \frac{z}{\sin\theta} \tag{3}$$

where b_w denotes the minimum web width and σ_{ctw} represents the principal tensile stress in concrete. The equation of vertical equilibrium leads to the expression of the shear force V in terms of the vertical projections of the contributions in (2) and (3), namely

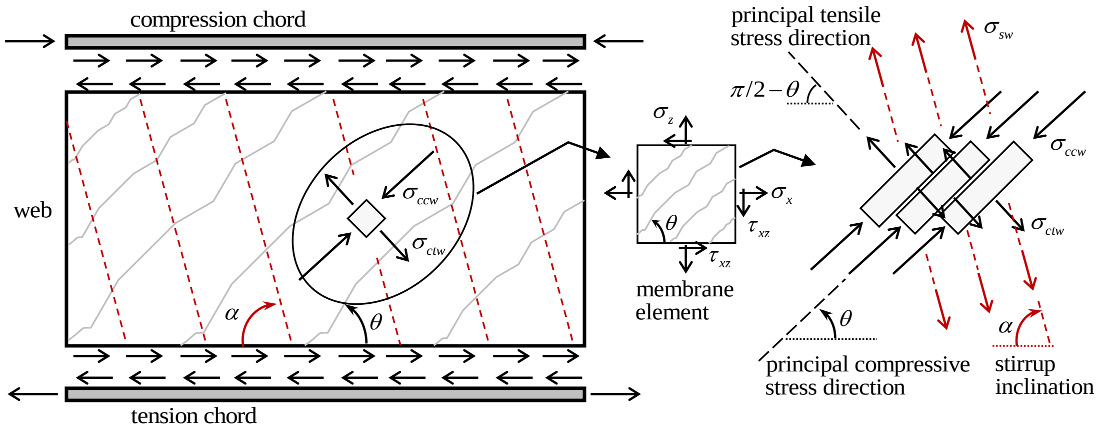

Fig. 1 Stress fields in a segment of a reinforced concrete beam

$$\begin{aligned} V &= S_{s1v} + S_{ct1v} = S_{s1}\sin\alpha + S_{ct}\cos\theta \\ &= \sigma_{sw} A_{sw}\frac{z(\cot\theta+\cot\alpha)}{s}\sin\alpha + \sigma_{ctw} b_w z\cot\theta \\ &= \left[\frac{\sigma_{sw}}{f_{ywd}}\omega_w(\cot\theta+\cot\alpha)\sin^2\alpha + \frac{\sigma_{ctw}}{\nu_1 f_{cd}}\cot\theta\right] b_w z \nu_1 f_{cd} \end{aligned} \quad (4)$$

in which the mechanical ratio of transverse reinforcement ω_w has been introduced, which is defined as follows (Reineck *et al.* 2014)

$$\omega_w = \frac{A_{sw} f_{ywd}}{b_w s \nu_1 f_{cd}\sin\alpha}. \quad (5)$$

In Eq. (4) and (5) f_{ywd} represents the design yield strength of transverse reinforcement, f_{cd} is the design concrete compressive strength and ν_1 is an efficiency factor for concrete cracked in shear whose value is typically in the range 0.5-0.6 (Reineck *et al.* 2014, EC2 2005). In the limit condition $\sigma_{sw} = f_{ywd}$ and $\sigma_{ctw} = \nu_2 f_{cd}$ (ν_2 being another efficiency factor for tensile stresses), Eq. (4) produces the shear strength due to contemporaneous yielding of steel transverse reinforcement combined with principal tensile stresses of concrete

$$V_{Rd1} = b_w z \nu_1 f_{cd}\left[\omega_w(\cot\alpha+\cot\theta)\sin^2\alpha + \mu\cot\theta\right] \quad (6)$$

where $\mu = \nu_2/\nu_1$ is a coefficient accounting for the biaxial failure of concrete membrane in plane stress state, typically in the range $1-6\%$ based on experimental findings (Menétrey and Willam 1995). The occurrence of this first failure mechanism (mainly ascribed to yielding of stirrups) is likely to occur for low amounts of transverse reinforcement.

For the second failure mechanism, let us consider the vertical equilibrium across another beam segment obtained through a section parallel to the stirrup inclination α, see Fig. 3. The stress fields contributing to this failure mechanism are both the principal tensile and compressive stresses of concrete. Let σ_{ccw} denote the uniform compressive stress field of concrete in the web of the beam (principal compressive stresses), while S_{cc2} indicates the corresponding resultant compressive force given by

$$\begin{aligned} S_{cc2} &= \sigma_{ccw} b_w \overline{AD} = \sigma_{ccw} b_w \overline{AB}\sin(\pi-\alpha-\theta) \\ &= \sigma_{ccw} b_w \frac{z}{\sin\alpha}\sin(\alpha+\theta). \end{aligned} \quad (7)$$

Similarly, let σ_{ctw} denote the uniform tensile stress field of concrete in the web of the beam (principal tensile stresses), while S_{ct2} indicates the corresponding resultant tensile force given by

$$\begin{aligned} S_{ct2} &= \sigma_{ctw} b_w \overline{BD} = \sigma_{ctw} b_w \overline{AB}\cos(\pi-\alpha-\theta) \\ &= -\sigma_{ctw} b_w \frac{z}{\sin\alpha}\cos(\alpha+\theta). \end{aligned} \quad (8)$$

The equation of vertical equilibrium leads to the expression of the shear force V in terms of the vertical projections of the contributions in (7) and (8), namely

$$\begin{aligned} V &= S_{cc2v} + S_{ct2v} = S_{cc2}\sin\theta + S_{ct2}\cos\theta \\ &= \left[\sigma_{ccw}\sin(\alpha+\theta)\sin\theta - \sigma_{ctw}\cos(\alpha+\theta)\cos\theta\right] b_w \frac{z}{\sin\alpha} \\ &= \left[\frac{\sigma_{ccw}}{\nu_1 f_{cd}}\frac{\sin(\alpha+\theta)}{\sin\alpha}\sin\theta - \frac{\sigma_{ctw}}{\nu_1 f_{cd}}\frac{\cos(\alpha+\theta)}{\sin\alpha}\cos\theta\right] b_w z \nu_1 f_{cd} \end{aligned} \quad (9)$$

In the limit condition $\sigma_{ccw} = \nu_1 f_{cd}$ and $\sigma_{ctw} = \nu_2 f_{cd}$, Eq. (9) produces the shear strength due to biaxial failure of the concrete membrane (combined principal compressive stresses and principal tensile stresses of concrete in the web of the beam)

$$V_{Rd2} = b_w z \nu_1 f_{cd}\left[\frac{\sin(\alpha+\theta)}{\sin\alpha}\sin\theta - \mu\frac{\cos(\alpha+\theta)}{\sin\alpha}\cos\theta\right] \quad (10)$$

which can be re-written in terms of cotangent functions exploiting simple trigonometric identities

$$V_{Rd2} = b_w z \nu_1 f_{cd}\left[\frac{\cot\theta+\cot\alpha}{\cot^2\theta} + \mu\frac{\cot\theta-\cot^2\theta\cot\alpha}{\cot^2\theta}\right] \quad (11)$$

The occurrence of this second failure mechanism is likely to occur for high amounts of transverse reinforcement, whereby the biaxial failure of concrete membrane occurs prior to stirrup yielding.

Finally, for the third failure mechanism let us consider vertical equilibrium across another beam segment obtained

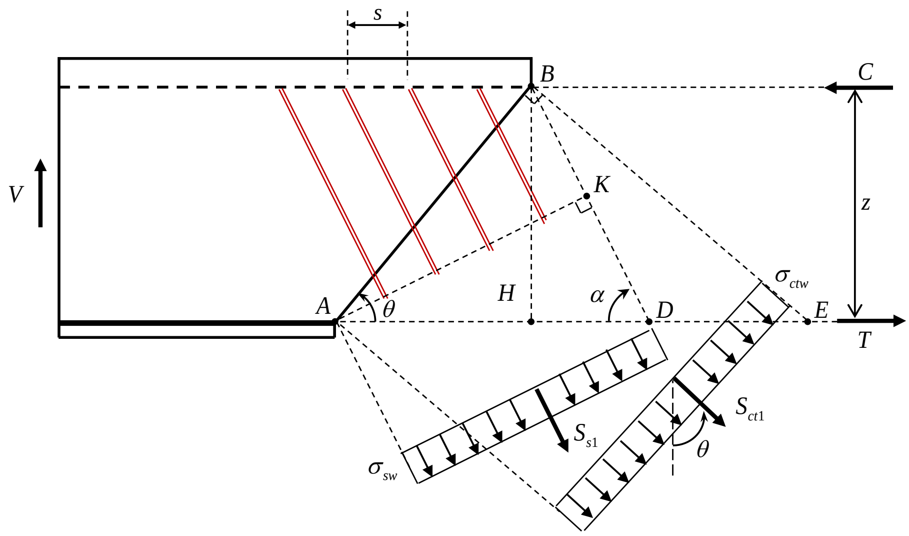

Fig. 2 First failure mechanism identified by a section parallel to the principal compressive stress direction (tensile stresses of stirrups and principal tensile stresses of concrete)

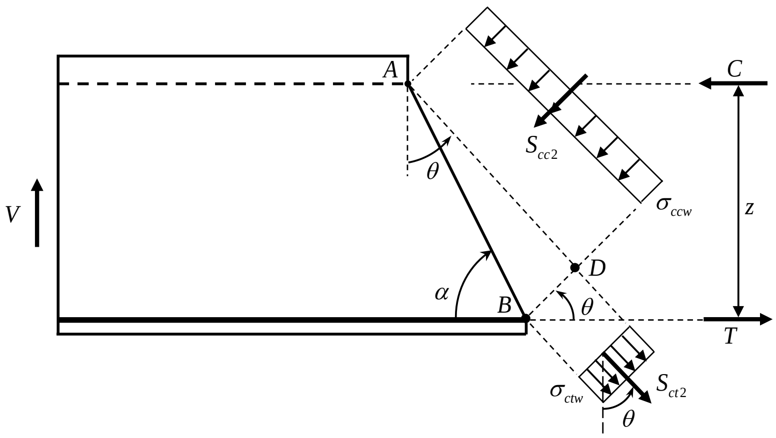

Fig. 3 Second failure mechanism identified by a section parallel to the stirrup inclination (principal compressive and tensile stresses of concrete)

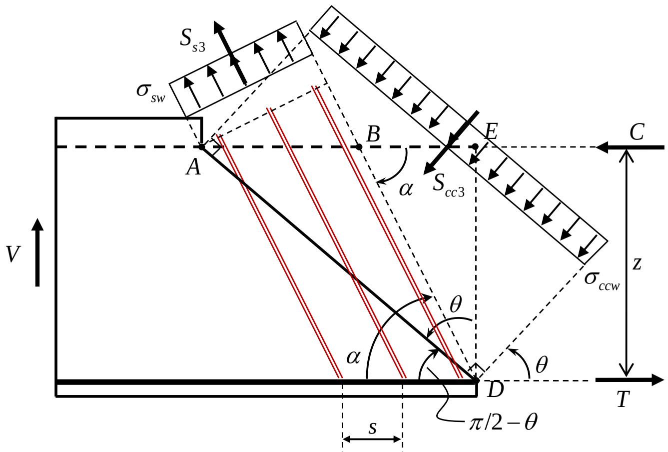

Fig. 4 Third failure mechanism identified by a section parallel to the principal tensile stress direction (principal compressive stresses of concrete and tensile stresses of stirrups)

through a section parallel to the principal tensile stress direction $\pi/2-\theta$, see Fig. 4. The stress fields contributing to this failure mechanism are the principal compressive stresses of concrete and the tensile stresses of stirrups. Let σ_{ccw} denote the uniform stress field of concrete in the web of the beam (principal compressive stresses), while S_{cc3} indicates the corresponding resultant compressive force given by

$$S_{cc3}=\sigma_{ccw}b_w\overline{AD}=\sigma_{ccw}b_w\frac{z}{\cos\theta} \tag{12}$$

As said above, in this section a contribution of stirrups in tension is also present. This contribution is proportional to the number of stirrups crossing the beam segment $\overline{AB}$, which is computed again under the hypothesis of a constant spacing s as in the first failure mechanism

$$n_{s3} = \frac{\overline{AB}}{s} = \frac{\overline{AE} - \overline{BE}}{s} = \frac{z(\tan\theta - \cot\alpha)}{s} \tag{13}$$

from which the resultant tensile force of the transverse reinforcement is given by

$$S_{s3} = \sigma_{sw} A_{sw} n_{s3} = \sigma_{sw} A_{sw} \frac{z(\tan\theta - \cot\alpha)}{s} \tag{14}$$

The equation of vertical equilibrium leads to the expression of the shear force V in terms of the vertical projections of the contributions in (12) and (14), namely

$$\begin{aligned} V &= S_{cc3v} + S_{s3v} = S_{cc3}\sin\theta - S_{s3}\sin\alpha \\ &= \sigma_{ccw} b_w \frac{z}{\cot\theta} - \sigma_{sw} A_{sw} \frac{z(\tan\theta - \cot\alpha)}{s}\sin\alpha \\ &= \left[\frac{\sigma_{ccw}}{\nu_1 f_{cd}} \frac{1}{\cot\theta} - \frac{\sigma_{sw}}{f_{ywd}} \omega_w (\tan\theta - \cot\alpha)\sin^2\alpha\right] b_w z \nu_1 f_{cd} \end{aligned} \tag{15}$$

In the limit condition $\sigma_{sw} = f_{ywd}$ and $\sigma_{ccw} = \nu_1 f_{cd}$, therefore Eq. (15) produces the shear strength due to contemporaneous yielding of steel transverse reinforcement combined with principal compressive stresses of concrete

$$V_{Rd3} = b_w z \nu_1 f_{cd} \left[\frac{1}{\cot\theta} - \omega_w \left(\frac{1}{\cot\theta} - \cot\alpha\right)\sin^2\alpha\right] \tag{16}$$

This failure mechanism involves both concrete in compression and steel in tension, therefore it is not easy to clearly identify the situations in which it is likely to occur.

In the sequel of the paper, dimensionless expressions are used to facilitate the application of the stress field formulation for practical design purposes. To this aim, the three expressions (6), (11) and (16) of the three failure mechanisms are divided by a normalization factor $r = b_w z \nu_1 f_{cd}$ (having dimension of force) to obtain the following dimensionless counterparts

$$v_{Rd1} = \frac{V_{Rd1}}{r} = \omega_w (\cot\alpha + \cot\theta)\sin^2\alpha + \mu\cot\theta \tag{17}$$

$$v_{Rd2} = \frac{V_{Rd2}}{r} = \frac{(\cot\theta + \cot\alpha)}{\cot^2\theta} + \mu\frac{(\cot\theta - \cot^2\theta\cot\alpha)}{\cot^2\theta} \tag{18}$$

$$v_{Rd3} = \frac{V_{Rd3}}{r} = \frac{1}{\cot\theta} - \omega_w \left(\frac{1}{\cot\theta} - \cot\alpha\right)\sin^2\alpha \tag{19}$$

which are the general expressions of the shear capacity of the proposed stress field limit analysis approach for an arbitrary angle α of the transverse reinforcement. In the following Section, these expressions are particularized for the common case of vertical stirrups ($\alpha = 90°$) and are compared to the expressions reported in the Eurocode 2.

3. Stress field limit analysis approach for vertical stirrups

In the case of vertical stirrups ($\alpha = 90°$), the expressions (17)-(19) can be simplified as follows

$$v_{Rd1} = (\omega_w + \mu)\cot\theta \tag{20}$$

$$v_{Rd2} = \frac{\cot\theta}{1+\cot^2\theta}(1+\mu) \tag{21}$$

$$v_{Rd3} = \frac{1}{\cot\theta}(1-\omega_w) \tag{22}$$

By inspection of expressions (20)-(22) the following critical considerations can be made:

1. The proposed stress field approach that includes the principal tensile stresses of concrete in an explicit manner represents a general case of the Eurocode 2 truss model. Indeed, the expressions of $v_{Rd,s}$ (failure due to yielding of stirrups) and $v_{Rd,c}$ (failure due to crushing of compressive struts) of the EC-2 model are retrieved as special cases of the expressions of v_{Rd1} and v_{Rd2}, respectively, in the limit condition $\mu = 0$, which implies that the contribution of the principal tensile stresses to the shear capacity is not taken into account;
2. The principal tensile stresses modify the two failure mechanisms incorporated in the EC-2 formulation, namely yielding of stirrups (failure mechanism 1) and crushing of compressive struts (failure mechanism 2) through an additional term linearly proportional to μ;
3. Incorporating the principal tensile stresses into the stress field approach gives rise to an additional failure mechanism that is not considered in the EC-2 model, namely the failure mechanism 3 obtained through a section parallel to the principal tensile stress direction;
4. The shear strength due to failure mechanism 1 is a linear function of the variable $\cot\theta$ (similarly to the EC-2 approach), whereas the shear strength of the other two failure mechanisms exhibits a nonlinear dependence upon the cotangent function of the angle θ;
5. The additional parameter μ quantifies the contribution of the principal tensile stresses to the shear capacity and should be calibrated based on biaxial failure envelope of concrete in the web of the beam as well as experimental considerations.

The actual shear strength is the smallest value of v_{Rd1}, v_{Rd2}, v_{Rd3}, that is

$$v_{Rd} = v_{Rd}(\omega_w, \mu, \theta) = \min(v_{Rd1}, v_{Rd2}, v_{Rd3}) \tag{23}$$

In line with the variable strut inclination method of the EC-2, which is based on the static theorem of limit analysis (Nielsen and Hoang 1999), the rational design method leads to assuming a value of $\theta = \theta_u$ (ultimate inclination angle of compression strut) corresponding to the simultaneous attainment of the three different failure mechanisms, namely

$$v_{Rd1}(\theta_u) = v_{Rd2}(\theta_u) = v_{Rd3}(\theta_u) \tag{24}$$

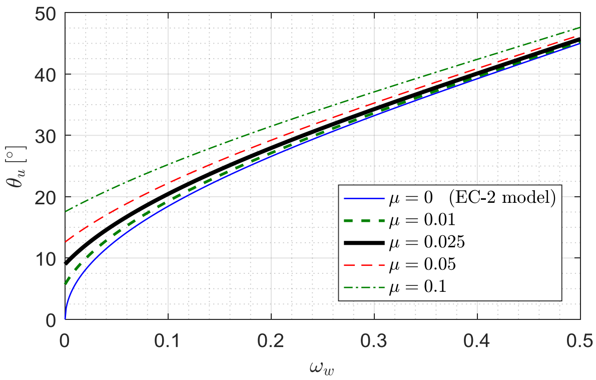

Fig. 5 Ultimate inclination angle of compression strut θ_u versus mechanical ratio of transverse reinforcement for different values of the tensile stress ratio μ

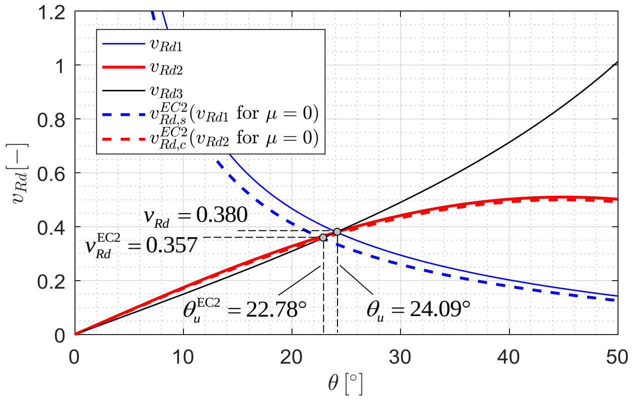

Fig. 6 Plot of the three failure mechanisms of the proposed stress field approach (for $\omega_w = 0.15$ and $\mu = 0.02$) compared to the two failure mechanisms of the EC-2 truss model ($\mu = 0$)

where the dependence upon the variables ω_w, μ has been omitted for compactness. The value of θ_u from (24) is given by

$$\theta_u = \cot^{-1}\sqrt{\frac{1-\omega_w}{\omega_w + \mu}} \tag{25}$$

This assumption maximizes the shear strength of the RC beam within the class of statically admissible (i.e., satisfying the equilibrium conditions) and plastically admissible (i.e., nowhere violating the yield conditions) solutions. The corresponding shear capacity can be obtained by substitution of the ultimate inclination angle (25) into one of the three expressions (as the three failure mechanisms are equivalent for $\theta = \theta_u$ due to Eq. (24)), which leads to

$$v_{Rd} = \sqrt{(\omega_w + \mu)(1-\omega_w)} \tag{26}$$

It can be seen that the ultimate inclination angle of the compression struts θ_u, given by (25) and plotted in Fig. 5 for a range of μ ratios, increases with the increase of the shear reinforcement ratio ω_w and with the increase of the tensile stress ratio μ. Moreover, for $\omega_w = 0$ the angle θ_u is not zero as in the EC-2 approach ($\mu = 0$), but equal to a fixed value given by $\cot^{-1}\left(\mu^{-\frac{1}{2}}\right)$.

Additional considerations of the different failure mechanisms of the proposed stress field approach (compared to the EC-2 truss model) can be made by referring to Fig. 6. The three failure mechanism curves of the proposed stress field approach are plotted for $\omega_w = 0.15$ and $\mu = 0.02$. Additionally, the two failure mechanisms of the EC-2 approach ($v_{Rd,s}$ and $v_{Rd,c}$, obtained from v_{Rd1} and v_{Rd2} in the limit case $\mu = 0$) are superimposed in the plot for comparative purposes and reported as dashed lines.

The following remarks can be made:

- For the assumed values of ω_w and μ, the third failure mechanism (curve v_{Rd3}) intersects the other two failure mechanisms of the proposed stress field model (v_{Rd1} and v_{Rd2}) at an angle $\theta_u = 24.09°$ (given by Eq. (25)), in other words for this value of strut inclination angle all the three failure mechanisms occur simultaneously;
- Interestingly, the third failure mechanism (curve v_{Rd3}) also intersects the two failure mechanisms of the EC-2 model ($v_{Rd,s}$ and $v_{Rd,c}$), which means that the additional considered third failure mechanism, whenever incorporated in the EC-2 formulation, would lead to the same value of ultimate inclination angle of the compression struts and, consequently, to the same expression of the shear capacity as in the Eurocode 2;
- For the assumed values of ω_w and μ, the intersection of the two failure mechanisms of the EC-2 approach occurs at $\theta_u^{\mathrm{EC2}} = 22.78°$, (given by Eq. (25) for $\mu = 0$), which is lower than $\theta_u = 24.09°$ identified in the proposes stress field approach; in other words, the presence of the principal tensile stresses of concrete slightly increases the ultimate inclination angle of the compression struts compared to the EC-2 formulation;
- Obviously, the shear capacity obtained in the proposed stress field approach that incorporates the principal tensile stresses of concrete is higher than that obtained without including this term in the equilibrium equations (EC-2 model); for the assumed values of ω_w and μ, the ordinate of the intersection point of the three failure mechanisms (continuous lines) is $v_{Rd} = 0.380$ (obtained by Eq. (26)), whereas for the EC-2 model the intersection of the two failure mechanisms (dashed lines) corresponds to $v_{Rd}^{\mathrm{EC2}} = 0.357$, therefore there is an increase of around 6% in terms of shear strength. Although this seems to be a modest strength increase, it strictly depends upon the selected input parameters ω_w and μ of this example. More significant strength increases (up to 40%) can be observed for other parameter combinations, as shown below.

Indeed, the increase of shear capacity is obviously related to the contribution of the principal tensile stresses, quantified by the parameter μ. In Fig. 7 this strength increase is illustrated for a range of μ ratios (the same range used in Fig. 5 for the ultimate inclination angle).

However, in the EC-2 model the variability of the strut inclination angle θ is limited in order to prevent large cracks in serviceability conditions (Thürlimann 1978). In particular, the following lower- bound and upper-bound

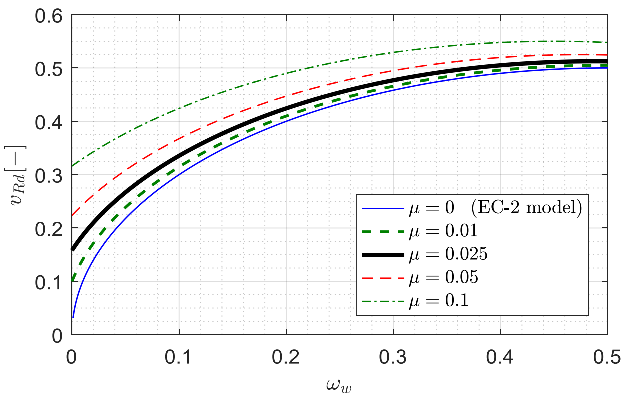

Fig. 7 Plot of the shear strength according of the proposed stress field approach for different values of the tensile stress ratio μ

limitations are imposed on the $\cot\theta$ variable

$$(\cot\theta)_{\min} \leq \cot\theta \leq (\cot\theta)_{\max} \tag{27}$$

These limitations are different from country to country, as overviewed in (Grandić *et al.* 2015). For the Eurocode 2 $(\cot\theta)_{\min} = 1$ and $(\cot\theta)_{\max} = 2.5$, which correspond to $21.8° \leq \theta \leq 45°$. This range is appropriate also for the proposed stress field approach, because it is likewise based on equilibrium principles and the lower-bound theorem of plasticity. Introducing the upper-bound limitation $(\cot\theta)_{\max} = 2.5$ into the expression of the ultimate inclination angle θ_u in (25) gives a value of $\omega_w = \omega_{w\lim}$ expressed by

$$\omega_{w\lim} = \frac{1}{29}(4 - 25\mu) = 0.1379 - 0.8621\mu \tag{28}$$

which identifies two different design regions (as in the EC-2 approach), the former (for $\omega_w < \omega_{w\lim}$) where the ultimate inclination angle is set equal to its lower-bound limit $\theta_u = \theta_{\min} = 21.8°$, and the latter (for $\omega_w \geq \omega_{w\lim}$) where the ultimate inclination angle θ_u can be varied in the range $21.8° \leq \theta \leq 45°$ according to Eq. (25) depending on the amount of shear reinforcement. The function $\omega_{w\lim}(\mu)$ for $\mu = 0$ (where the principal tensile stress contribution is neglected) gives $\omega_{w\lim} = 0.1379$, which represents the value of the EC-2 approach, while for $\mu > 0$ this limit value of transverse reinforcement identifying the two design regions decreases linearly.

In Fig. 8 the failure mechanisms are plotted for $\mu = 0.02$ and for a value of $\omega_w < \omega_{w\lim}$, namely $\omega_w = 0.05$. It is reasonable to notice that for low amounts of transverse reinforcement (design scenarios in which $\omega_w < \omega_{w\lim}$) the shear strength is controlled by yielding of stirrups, because the lowest shear capacity (which is the actual failure mechanism that is activated) is offered by the first failure mechanism v_{Rd1} due to yielding of stirrups in combination with principal tensile stresses of concrete. This also occurs in the EC-2 approach, where the failure is ascribed to $v_{Rd,s}$, i.e., to the occurrence of yielding of stirrups. Consequently, when $\omega_w < \omega_{w\lim}$, the shear capacity is given by

$$v_{Rd} = v_{Rd1}\big|_{\cot\theta = (\cot\theta)_{\max}} = 2.5(\omega_w + \mu) \tag{29}$$

which is a linear function of the mechanical ratio of transverse reinforcement. The corresponding trend of the shear strength for the unconstrained (without limitations on θ) and constrained case (taking into account the conditions in (27)) is shown in Fig. 9.

For $\omega_w = 0$ the residual shear capacity is offered by a term dependent upon the tensile stress ratio μ – this shear capacity is somehow related to the shear strength of the RC beam without transverse reinforcement, given by the tensile stress contribution of concrete.

Nevertheless, it is worth noting that more complicated mechanisms, like dowel action, aggregate interlock and residual tensile stresses take place in the beam (ACI 445R-99; Olalusi 2019), which are not fully included here. For this reason, the proposed stress field approach is considered valid only for RC beams with stirrups, namely for $\omega_w > 0$. In this regard, Eq. (29) is applicable only to a value of ω_w greater than the minimum value of transverse reinforcement as reported in §9.2.2 of the EC2 (2005), depending on the class of steel and concrete. On the other hand, introducing the lower-bound limitation $(\cot\theta)_{\min} = 1$ into the expression of the ultimate inclination angle θ_u in (25) gives a value of $\omega_w = \omega_{w\max}$ expressed by

$$\omega_{w\max} = \frac{1-\mu}{2} \tag{30}$$

which is again a modification of the EC-2 value ($\omega_{w\max} = 1/2$) due to the presence of the tensile stress ratio μ. Expression (30) implies that the maximum value of the shear capacity (maximum value of the parabola represented by Eq. (21)) is attained for a value of ω_w that is lower than 0.5. From this point onwards, a further increase of the shear reinforcement is useless, because web crushing of concrete (combined with principal tensile stresses) governs the shear failure in this range, with a constant strut inclination angle equal to 45° and corresponding shear capacity given by

$$v_{Rd\max} = \frac{1}{2}(1+\mu) \tag{31}$$

Overall, the proposed stress field approach modifies the design parameters of the EC-2 truss model due to the presence of the tensile stress ratio μ. Comparison of the main parameters of the two approaches is summarized in Table 1.

4. Comparison with experimental results

The proposed stress field approach is validated against published experimental results from the literature. Many shear strength databases were reported in the literature by various authors, such as (Lee *et al.* 2011, Zhang *et al.* 2015, Mansour *et al.* 2004). In this work, the databases selected by a joint ACI-DafStb group and published by Reineck *et al.* (2014, 2017) are adopted, which concern slender beams with vertical stirrups subjected to point loads. These databases are chosen because of the underlying clear and

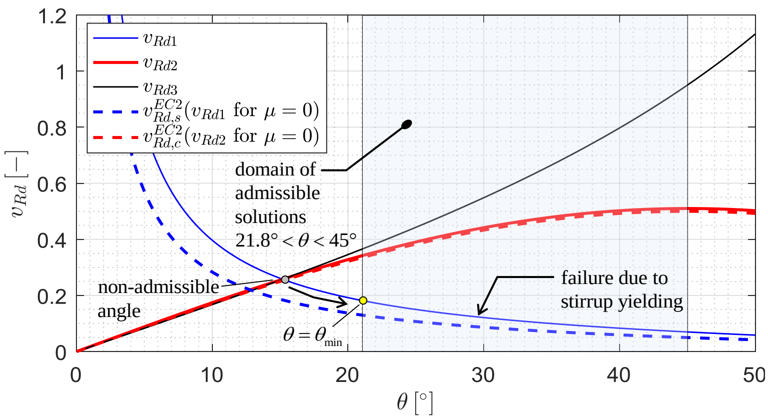

Fig. 8 Identification of the shear strength for design scenarios in which $\omega_w < \omega_{w\lim}$

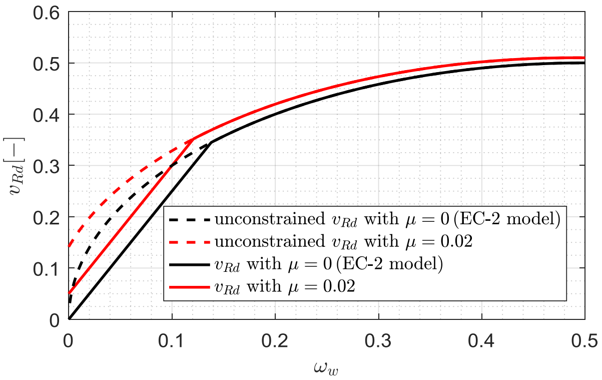

Fig. 9 Plot of the shear strength according of the proposed stress field approach for $\mu = 0.02$ and accounting for the limitations on the strut inclination angle given by Eq. (27)

transparent control criteria used to minimize the influence of database heterogeneity. Some of these criteria involved, for instance, slenderness ratios, minimum compressive strength, flexural checks, lack of mechanical or geometrical details in the original test reports, etc. Two databases are considered in this study, namely: 1) a smaller database reported in Reineck *et al.* (2014) and comprising 87 tests, 2) a larger database, which is a combination of the previous small database together with the ACI-DafStb H. 617 database Reineck *et al.* (2017), the latter comprising 170 tests. The larger database in 2) includes 213 independent tests, because 44 out of the 170 tests reported in the ACI-DafStb H. 617 database were also reported in the small evaluation database (therefore, only 126 tests of the ACI-DafStb H. 617 database are actually independent from the small evaluation database). Full details of the RC beams belonging to the two databases can be found in the original papers by Reineck *et al.* (2014, 2017).

In order to make a consistent comparison between experimental data and the proposed stress field approach as well as the Eurocode 2 model, over-reinforced beams are preliminarily identified. Based on the considerations by Lee and Hwang (2010), beams having $\omega_c = \rho_w f_{yw}/f_c > 0.2$ ($\rho_w = A_{sw}/(b_w s)$ denoting the transverse reinforcement ratio) are characterized by over-reinforced shear failure, with crushing of web concrete occurring prior to yielding of steel reinforcement. However, this is in contrast to the main assumptions made in Section 2 for the proposed plasticity-based approach. This aspect was also pointed out by other authors who used other plasticity-based approaches (He *et al.* 2015). In particular, 4 of the 87 beams in the small database, and 8 of the 213 beams in the large database have $\omega_c > 0.2$ and are, therefore, excluded in this comparison. It is worth noting that some of these over-reinforced beams also imply values of $\omega_c > 1.0$, which makes the expression (25) (for $\mu = 0$) complex-valued and, thus, physically meaningless. After eliminating these 4 and 8 beams in the two databases, the resulting reduced databases are formed by 83 and 205 beams, respectively, and the range of main geometrical and mechanical parameters is reported in Table 2.

In Fig. 10 the experimental shear strength data are reported in the $v - \omega_w$ plane. From the experimental shear strength $V_{\exp}$ the corresponding dimensionless value $v_{\exp}$ is calculated by dividing with $r = b_w z v_1 f_{cd}$. The efficiency factor v_1 has been computed as recommended by the Eurocode 2 (2005) through the formula $v_1 = 0.6(1 - f_c/250)$, which changes depending on the cylinder compressive strength of concrete. The $v - \omega_w$ curve of the Eurocode 2 truss model is reported as blue thin line in Fig. 10 and proves to be over-conservative throughout the range of transverse reinforcement ratios ω_w.

The over-conservativeness of the EC-2 approach was documented also by other researchers (Olalusi 2019, Zhang *et al.* 2015, He *et al.* 2015, Cladera and Marí 2007, De Domenico and Ricciardi 2019) considering different databases. On the other hand, since the proposed stress field approach introduces another strength parameter μ, different values of μ are investigated. The increase of shear capacity due to principal tensile stresses of concrete is expected to be more pronounced for higher amounts of transverse reinforcement. Indeed, for RC beams with higher shear reinforcement ratios, the crack widths are reduced and mainly controlled by the presence of stirrups. It is widely recognized that the contribution of residual tensile stresses in the web of the beam depends upon the crack width, and is more significant for smaller crack widths (ACI 445R-99). Based on these phenomenological considerations, the following expression of μ that is linearly increasing with ω_w is proposed.

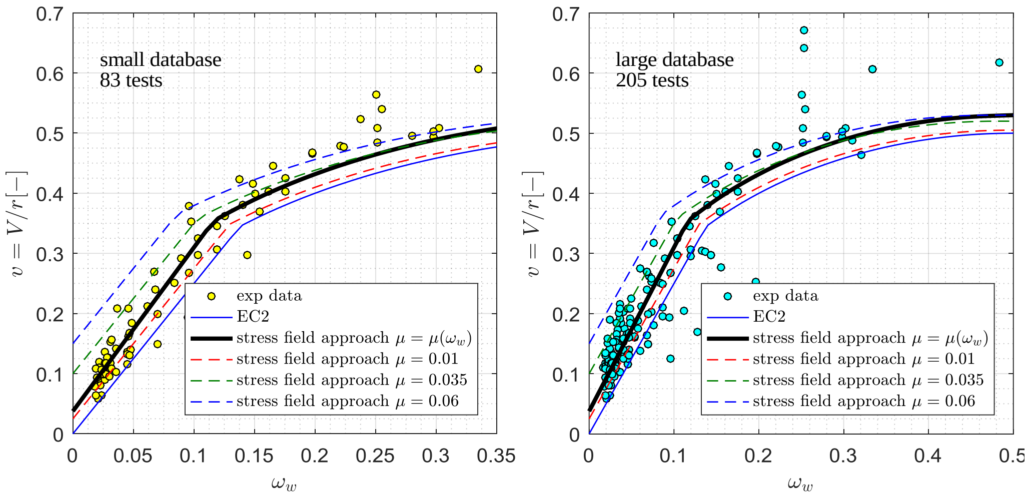

Fig. 10 Comparison of experimental shear strength versus predictions obtained with the proposed stress field approach with three values of μ and with $\mu = \mu(\omega_w)$ given in Eq. (32) as well as with the EC-2 model

$$\mu = 0.015(1 + 6\omega_w) \tag{32}$$

which is equal to 0.015 in the limit as $\omega_w \to 0$, and equal to 0.06 for $\omega_w = 0.5$. In this way, the phenomenological relationship $\mu = \mu(\omega_w)$ when incorporated into the proposed stress field approach increases the shear strength of the Eurocode 2 model depending on the mechanical ratio of transverse reinforcement ω_w. The shear strength curve of the proposed stress field approach with μ computed through Eq. (32) is reported in black solid line in Fig. 10.

Other three curves are superimposed as (red, green and blue) dashed lines and correspond to three fixed values of μ equal to 0.01, 0.035, and 0.06, respectively (i.e., not variable with the shear reinforcement ratio ω_w but assumed constant throughout the range of ω_w). It is clearly seen that the dashed line for $\mu = 0.01$ is in good agreement with the experimental points only for low values of ω_w, whereas it is over-conservative for higher amounts of shear reinforcement. On the other hand, the dashed line for $\mu = 0.06$ is relatively closer to the experimental results only for very high amounts of shear reinforcement, but is excessively under-conservative in the range $\omega_w < 0.2$ where most of the data fall. The derivation of the expression (32) is in fact based on these observations and allows capturing the variation of the shear strength with the increase of mechanical ratio of transverse reinforcement in an effective manner.

In order to highlight the better predictive performance of the proposed stress field approach with μ determined through Eq. (32) in comparison with alternative formulations based on a constant value of μ, in Fig. 11 the $v_{\text{exp}}/v_{\text{pred}}$ ratio is reported for the large database (205 tests) as a function of ω_w for different cases of μ. The same conclusions as above can be drawn, whereby a constant μ is able to capture the trend of the experimental data just for a limited range of ω_w, and does not achieve an acceptable predictive performance throughout the range of shear reinforcement ratios. The quantitative performance of the various variants of the stress field approach depending on the choice of the tensile stress ratio μ is summarized in Table 3 in terms of mean, standard deviation, coefficient of variation (CoV), minimum and maximum values of the $v_{\text{exp}}/v_{\text{pred}}$ ratio for the large database. The mean of proposed stress field approach with μ determined through Eq. (32) is 1.03, and the CoV is 21.93%. On the other hand, the other formulations are associated with mean greater than 1 (low values of μ) or lower than 1 (high values of μ) and higher values of CoV (worse precision).

Table 1 Main parameters of the proposed stress field approach compared to the EC-2 truss model

parameter	EC-2 approach	stress field approach
ω_{wlim}	0.1379	$0.1379 - 0.8621\mu$
$\omega_{w\max}$	1/2	$(1-\mu)/2$
$\cot\theta_u$	$\sqrt{(1-\omega_w)/\omega_w}$	$\sqrt{(1-\omega_w)/(\omega_w+\mu)}$
v_{Rd} for $\cot\theta_u > 2.5$ (design region 1)	$2.5\omega_w$	$2.5(\omega_w+\mu)$
v_{Rd} for $1 \le \cot\theta_u \le 2.5$ (design region 2)	$\sqrt{\omega_w(1-\omega_w)}$	$\sqrt{(\omega_w+\mu)(1-\omega_w)}$
v_{Rd} for $\cot\theta_u < 1$ (design region 3)	1/2	$(1+\mu)/2$

Table 2 Range of input parameters in the two considered databases

	ACI-DafStb small database (83 tests)		ACI-DafStb large database (205 tests)	
input parameter	min	max	min	max
$b_w(mm)$	50.0	457.2	50.0	457.2
$d(mm)$	198.0	1200.0	161.0	1200.0
$a/d(-)$	2.448	7.102	2.444	7.102
$\rho_w(\%)$	0.079	1.678	0.070	2.646
$f_{yw}(MPa)$	270.0	820.0	229.0	820.0
$f_c(MPa)$	15.7	125.3	13.4	125.3
ω_w	0.018	0.334	0.017	0.484
V_{exp}(kN)	94.0	1330.0	81.0	1330.0

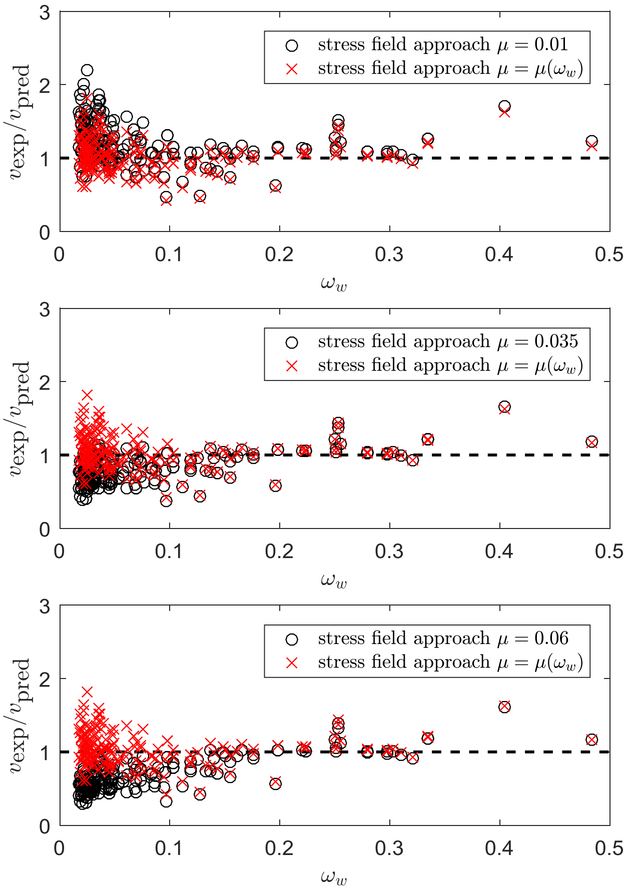

Fig. 11 Comparative trend of $v_{\text{exp}}/v_{\text{pred}}$ ratio versus ω_w for stress field approach with three values of μ and with $\mu = \mu(\omega_w)$ given in Eq. (32)

The proposed stress field approach is also compared to other code-based formulations, namely the EC2 (2005), the ACI 318-11 additive approach (2011) (the same approach as in ACI 318-18 regulations (2018)), and the Model Code 2010 level III (fib 2013), and the corresponding performance is illustrated in Fig. 12 and in Fig. 13 in the $v_{\text{pred}} - v_{\text{exp}}$ plane for the small and large databases, respectively. For the proposed stress field approach, most of the couples $(v_{\text{exp}}, v_{\text{pred}})$ reasonably fall along the 45° line and are equally distributed above and below the 45° line, which implies small bias and high accuracy, on average. In particular, an excellent predictive performance is achieved for the small database, with mean equal to 1.00 and CoV of 16.45%. It is worth noting that the code-based formulations are applied without any partial safety factor, using the mean values of the material strength parameters. Consequently, the results compared are not exactly the actual predictions of the different models, because characteristic or design values of the material strength parameters should be assumed depending on the model considered. However, as a general trend, the code-based formulations produce higher mean values, in the range 1.40-1.50 (meaning 40-50% of model safety factor, on average) and higher values of CoV (meaning lower precision) in comparison with the proposed model. As an example, the CoV of the Eurocode 2 is 30% higher than the CoV of the proposed stress field approach

Table 3 Predictive performance of stress field approach with three constant values of μ against proposed empirical formula $\mu = \mu(\omega_w)$ given in Eq. (32) for large database (205 tests)

$v_{\text{exp}}/v_{\text{pred}}$ ratio	$\mu = \mu(\omega_w)$	$\mu = 0.01$	$\mu = 0.035$	$\mu = 0.06$
mean	1.03	1.19	0.79	0.67
standard deviation	0.226	0.277	0.206	0.222
CoV (%)	21.93	23.23	26.12	33.33
minimum	0.42	0.47	0.37	0.29
maximum	1.82	2.20	1.65	1.62

for both the databases. Based on these comparisons, it can be concluded that the incorporation of the principal tensile stresses of concrete leads to a significant improvement of the Eurocode 2 model in terms of both accuracy (mean) and precision (CoV). The expression of μ proposed in Eq. (32) provides good agreement between predicted shear strength and experimental data. The introduction of the principal tensile stresses does not complicate the EC-2 formulation, and is directly incorporated in the expressions reported in Table 1, using the same theoretical principles as in the EC-2 model, namely equilibrium conditions and lower-bound theorem of plasticity.

As a final remark, it is worth noting that the ultimate inclination angle of the compression struts θ_u is a key parameter for the evaluation of the shear strength. In the proposed stress field approach, the angle θ_u is evaluated through the static theorem of limit analysis, and is based on the mechanical ratio of transverse reinforcement ω_w and the tensile stress ratio μ according to Eq. (25). However, if a one-to-one relation between ω_w and μ is assumed according to Eq. (32), the following nonlinear formula between ω_w and θ_u is obtained

$$\theta_u = \cot^{-1}\sqrt{\frac{1-\omega_w}{\omega_w + 0.015(1+6\omega_w)}} \tag{33}$$

which for any value of ω_w gives a unique value of θ_u.

The validity of Eq. (33) is checked against experimental results from the literature. It is rather difficult to carry out experimental measurements concerning the ultimate inclination angle of the principal compressive stresses in the web of the beam. However, by a proper arrangement of a series of LVDTs in triangles, it is possible to measure deformations of the web of the beam along different directions. Exploiting Mohr's circle principles, the inclination of the principal compressive strains can be determined accordingly. The assumption of principal compressive stress directions coincident with principal compressive strain directions was often made in other works from the literature (Vecchio and Collins 1986), although strictly speaking the former lag behind the latter. Under this assumption, it is possible to compare the θ_u values found through Eq. (33) with the inclination of principal compressive strain direction obtained from experimental measurements. A series of such measurements were performed by Walraven *et al.* (2013) for I-shaped

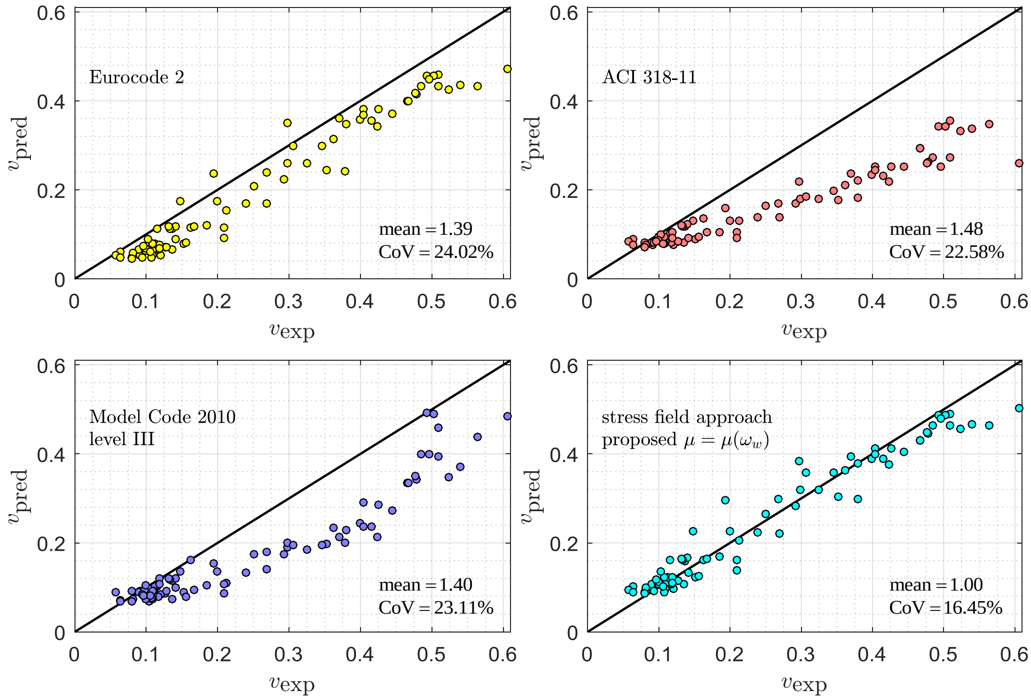

Fig. 12 Predicted versus experimental shear strength using various code formulations and the proposed stress field approach with $\mu = \mu(\omega_w)$ given in Eq. (32) for small database

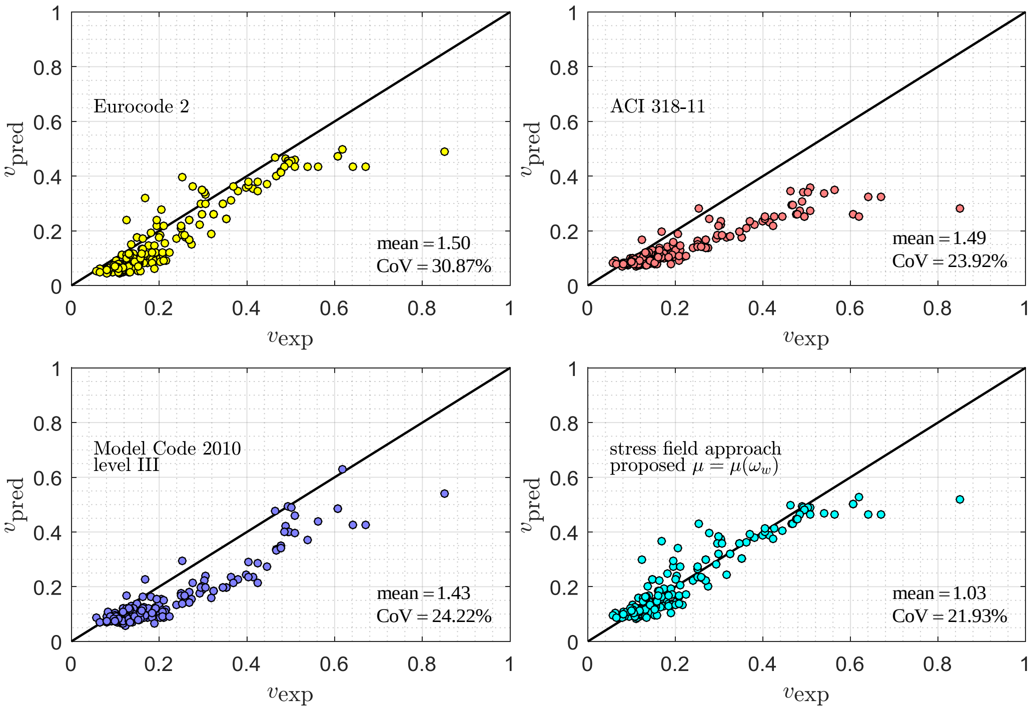

Fig. 13 Predicted versus experimental shear strength using various code formulations and the proposed stress field approach with $\mu = \mu(\omega_w)$ given in Eq. (32) for large database

beams having different shear reinforcement ratios, and the corresponding experimental results are reported in Fig. 14 as cyan dots. The solid curve superimposed in the plot is the trend described by Eq. (33) (predictions of the proposed stress field approach). Moreover, the ultimate inclination angles predicted by plasticity theory combined with MCFT, based on a variable-angle truss model proposed by He *et al.* (2015), is also reported in the plot for comparative purposes It is clearly seen that there is a reasonable agreement between predicted and experimental angles for both the proposed stress field approach and the plasticity theory + MCFT. In particular, for the proposed model the mean value of the ratio $\theta_{exp}/\theta_{predicted}$ is 0.92 and the CoV of the same ratio is 9.13%. The predictions of the proposed stress field approach are in very good agreement with the experimental results in the range $\omega_w < 0.3$, which is the most significant

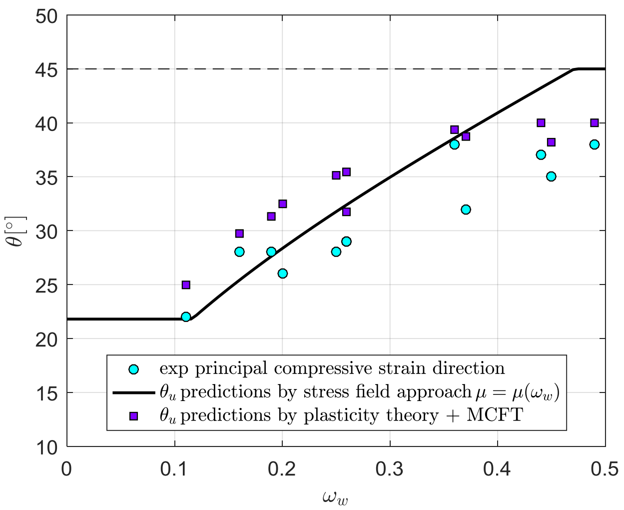

Fig. 14 Comparison between experimental and predicted strut inclination angles for I-shaped beams tested by Walraven *et al*. (2013)

range as more pronounced strut rotations are expected to occur for lower amounts of transverse reinforcement. As the stirrup ratio increases, the failure occurs with minimal strut rotation and the proposed stress field approach tends to slightly overestimate the inclination of the compressive stress direction.

5. Conclusions

A stress field limit analysis approach for the shear capacity of RC beams with stirrups has been elaborated. The model is based on the concept of cracked membrane element combined with the variable strut inclination method of the Eurocode 2. Unlike the EC-2 approach, the proposed model explicitly incorporates the contribution of the principal tensile stresses of concrete in the beam web. The proposed model and the corresponding shear strength expressions are based on simple equilibrium considerations on different beam segments. Three different failure mechanisms have been identified, and the ultimate strut inclination angle θ_u has been determined through the static theorem of limit analysis, maximizing the shear strength within the class of statically and plastically admissible solutions. The presence of principal tensile stresses slightly increases the ultimate strut inclination angle θ_u and is incorporated in the shear design expressions through a phenomenological expression that is linearly increasing with the mechanical ratio of transverse reinforcement ω_w. It has demonstrated that the proposed stress field limit analysis approach is in very good agreement with experimental shear strength results from the literature. In particular, a comparison with more than 200 experimental results from the literature has revealed an average ratio of experimental to predicted shear strength very close to unity (1.03), and a CoV in the range of 16-20%, which is around 30% lower than that corresponding to the Eurocode 2 approach. Moreover, the proposed stress field approach provides values of the ultimate strut inclination angles that are fairly in line with experimental measurements of principal compressive strain direction as well as in agreement with inclination angles predicted by other models reported in the literature.

References

ACI Commettee 318 (2011), *Building Code Requirements for Structural Concrete (ACI 318-11) and Commentary*, Farmington Hills, MI, USA.

ACI-ASCE Committee 445 (1998), “ACI 445R-99. Recent approaches to shear design of structural” concrete, *J Struct Eng*, **124**(12), 1375-1417. http://doi.org/10.1061/(ASCE)0733-9445(1998)124:12(1375).

Bach, F., Braestrup, M.W. and Nielsen, M.P. (1978), “Rational analysis of shear in reinforced concrete beams.”, *I.A.B.S.E. proceedings*, p. 15. http://doi.org/10.5169/seals-33219.

Cladera, A. and Marí, A.R. (2007), “Shear strength in the new Eurocode 2. A step forward?”, *Structural Concrete*, **8**(2), 57-66. http://doi.org/10.1680/stco.2007.8.2.57.

Collins, M., Bentz, E. and Sherwood, E. (2008), “Where is shear reinforcement required? Review of research results and design procedures”, *ACI Struct J*, **105**(5), 590-600.

CEB-FIP ’90 (1993), *Model Code for Concrete Structures for Buildings*, Comitè Eurointernational du Bèton, Lausanne, Switzerland.

De Domenico, D., Fuschi, P., Pardo, S. and Pisano, A.A. (2014), “Strengthening of steel-reinforced concrete structural elements by externally bonded FRP sheets and evaluation of their load carrying capacity”, *Compos. Struct.*, **118**(1), 377-338. https://doi.org/10.1016/j.compstruct.2014.07.040.

De Domenico, D., Faleschini, F., Pellegrino, C. and Ricciardi, G. (2018), “Structural behavior of RC beams containing EAF slag as recycled aggregate: Numerical versus experimental results”, *Constr. Build. Mater.*, **171**, 321-337. https://doi.org/10.1016/j.conbuildmat.2018.03.128.

De Domenico, D. and Ricciardi, G. (2019), “Shear strength of RC beams with stirrups using an improved Eurocode 2 truss model with two variable-inclination compression struts”, *Eng. Struct.*, **198**, 109359. https://doi.org/10.1016/j.engstruct.2019.109359.

DIN 1045-1 (2008), *Tragwerke aus Beton, Stahlbeton und Spannbeton* (in German), Normenauschuss Bauwesen (NABau) im DIN, Berlin, Germany.

EC2 (2005), *Eurocode No. 2. Design of Concrete Structures – Part. 1-1: General Rules and Rules for Buildings*, UNI EN 1992-1-1, 2005, European committee for standardisation, Brussels, Belgium.

ENV 1992-1-1 (1991), *Eurocode 2 - Design of Concrete Structures - Part 1-1: General Rules and Rules for Buildings*, European committee for standardisation, Brussels, Belgium.

Fédération Internationale du Béton (2013), *fib Model Code for Concrete Structures 2010*, International Federation for Structural Concrete (fib), Ernst & Sohn, 2013, Lausanne, Switzerland.

Fuschi, P., Pisano, A.A. and Weichert, D. (Eds.) (2015), *Direct Methods for Limit and Shakedown Analysis of Structures*. Springer, Berlin, Germany. http://doi.org/10.1007/978-3-319-12928-0.

Grandić, D., Šćulac, P. and Grandić, I.Š. (2015), “Shear resistance of reinforced concrete beams in dependence on concrete strength in compressive struts”, *Technical Gazette*, **22**(4), 925-934. http://doi.org/10.17559/TV-20140708125658.

He, Z.Q., Liu, Z. and John, Ma.Z. (2015), “Simplified shear design of slender reinforced concrete beams with stirrups”, *J Struct Eng*, **142**(2), 06015003. http://doi.org/10.1061/(ASCE)ST.1943-541X.0001394.

Hsu, T.T.C. (1988), “Softened truss model theory for shear and torsion", *ACI Struct. J.*, **85**(6), 624–635.

Kaufmann, W. and Marti, P. (1998), "Structural concrete: cracked membrane model", *J Struct Eng*, **124**(12), 1467-1475. https://doi.org/10.1061/(ASCE)0733-9445(1998)124:12(1467).

Keskin, R.S. (2017), "Predicting shear strength of SFRC slender beams without stirrups using an ANN model", *Struct. Eng. Mech.*, **61**(5), 605-615. http://dx.doi.org/10.12989/sem.2017.61.5.605.

Le, C.V., Gilbert, M. and Askes, H. (2010), "Limit analysis of plates and slabs using a meshless equilibrium formulation", *Int. J. Numer. Meth. Eng.*, **83**(13), 1739–1758. https://doi.org/10.1002/nme.2887.

Le, C.V., Nguyen, P.H., Askes, H. and Pham, D.C. (2017), "A computational homogenization approach for limit analysis of heterogeneous materials", *Int. J. Numer. Meth. Eng.*, **112**(10), 1381-1401. https://doi.org/10.1002/nme.5561.

Lee, J.Y., Choi, I.J. and Kim, S.W. (2011), "Shear behavior of reinforced concrete beams with high-strength stirrups", *ACI Struct. J.*, **108**(5), 620–629.

Lee, J.Y. and Hwang, H.B. (2010), "Maximum shear reinforcement of reinforced concrete beams", *ACI Struct. J.*, **107**(5), 580–588.

Leonhardt, F. (1973), *Vorlesungen über Massivbau – Erster Teil*, Springer-Verlag GmbH, Berlin, Germany.

Li, B. and Tran, C.T.N. (2012), "Determination of inclination of strut and shear strength using variable angle truss model for shear-critical RC beams", *Struct. Eng. Mech.*, **41**(4), 459-477. http://dx.doi.org/10.12989/sem.2012.41.4.459.

Limam, O., Foret, G. and Ehrlacher, A. (2003a), "RC beams strengthened with composite material: a limit analysis approach and experimental study", *Compos. Struct.*, 59, 467–472. https://doi.org/10.1016/S0263-8223(02)00286-6.

Limam, O., Foret, G. and Ehrlacher, A. (2003b), "RC two-way slabs strengthened with CFRP strips: experimental study and a limit analysis approach", *Compos. Struct.*, **60**(4), 467-471. https://doi.org/10.1016/S0263-8223(03)00011-4.

Londhe, R.S. (2009), "The design of reinforced concrete beams for shear in current practice: A new analytical model", *Struct. Eng. Mech.*, **31**(2), 225-235. http://dx.doi.org/10.12989/sem.2009.31.2.225.

Mansour, M.Y., Dicleli, M., Lee, J.Y. and Zhang, J. (2004), "Predicting the shear strength of reinforced concrete beams using artificial neural networks", *Eng Struct*, **26**(6), 781-799. https://doi.org/10.1016/j.engstruct.2004.01.011.

Marti, P. (1985), "Basic tools of reinforced concrete beam design", *ACI Struct J*, **82**(1), 46-56.

Menétrey, P. and Willam, K.J. (1995) "A triaxial failure criterion for concrete and its generalization", *ACI Struct. J.*, **92**, 311-318.

Mörsch, E. (1908), *Der Eisenbetonbau. Seine Theorie und Anwendung*, Stuttgart: Wittwer, Germany.

Nielsen, M.P., Hoang, L. (1999), *Limit analysis and concrete plasticity*, 2nd ed., CRC, Florida, USA.

NTC18 (2018), *D.M. LL. PP. 17 Gennaio 2018. Aggiornamento delle «Norme tecniche per le costruzioni»*, (in Italian), Ministero delle Infrastrutture e dei Traporti, Rome, Italy.

Olalusi, O.B. (2019), "Present State of Eurocode 2 Variable Strut Inclination Method for Shear Design and Possible Improvement", *Structures*, **19**, 48-57. https://doi.org/10.1016/j.istruc.2018.11.016.

Park, M.K., Lee, D.H., Ju, H., Hwang, J.H., Choi, S.H. and Kim, K.S. (2015). "Minimum shear reinforcement ratio of prestressed concrete members for safe design", *Struct. Eng. Mech.*, **56**(2), 317-340. http://dx.doi.org/10.12989/sem.2015.56.2.317.

Park, R. and Paulay, T. (1975), *Reinforced Concrete Structures*, John Wiley and Sons, New York, USA.

Pisano, A.A., Fuschi, P. and De Domenico, D. (2013), "A kinematic approach for peak load evaluation of concrete elements", *Comput. Struct.*, **119**, 125-139. https://doi.org/10.1016/j.compstruc.2012.12.030.

Pisano, A.A., Fuschi, P. and De Domenico, D. (2015), "Numerical limit analysis of steel-reinforced concrete walls and slabs", *Comput. Struct.*, **160**, 42-55. https://doi.org/10.1016/j.compstruc.2015.08.004.

Qissab, M. and Salman, M.M. (2018), "Shear strength of non-prismatic steel fiber reinforced concrete beams without stirrups", *Struct. Eng. Mech.*, **67**, 347-358. http://dx.doi.org/10.12989/sem.2018.67.4.347.

Regan, P.E. (1969), "Shear in reinforced concrete beams", *Magazine of Concrete Research*, **21**(66), 31-42. https://doi.org/10.1680/macr.1969.21.66.31.

Reineck, K.H., Bentz, E., Fitik, B., Kuchma, D.A. and Bayrak, O. (2014), "ACI-DAfStb Databases for Shear Tests on Slender Reinforced Concrete Beams with Stirrups", *ACI Struct J*, **111**(5), 1147-1156.

Reineck, K.H. and Dunkelberg, D. (2017), *ACI-DAfStb databases 2015 on shear tests for evaluating relationships for the shear design of structural concrete members without and with stirrups*, Report for Research Project DAfStb V479. Reineck K-H, Dunkelberg, D. (Eds.). Beuth Verl. Berlin, Germany.

Ritter, W. (1989), "Die Bauweise Hennebique", *Schweizerische Bauzeitung*, **33**(7), 59-66.

Russo, G., Mitri, D. and Pauletta, M. (2013), "Shear strength design formula for RC beams with stirrups", *Eng. Struct.*, **51**: 226-235. https://doi.org/10.1016/j.engstruct.2013.01.024.

Russo, G. and Puleri, G. (1997), "Stirrup effectiveness in reinforced concrete beams under flexure and shear", *ACI Struct. J.*, **94**(3), 451-476.

Sigrist, V. (2011), "Generalized Stress Field Approach for Analysis of Beams in Shear", *ACI Struct. J.*, **108**(4), 497-487.

Sigrist, V., Bentz, E., Fernández-Ruiz, M., Foster, S. and Muttoni, A. (2013), "Background to the fib Model Code 2010 shear provisions–part I: beams and slabs", *Struct. Concr.*, **14**(3), 195-203. https://doi.org/10.1002/suco.201200066.

Spiliopoulos, K. and Weichert, D. (Eds.) (2014), *Direct Methods for Limit States in Structures and Materials*, Springer, Berlin, Germany. https://doi.org/10.1007/978-94-007-6827-7.

Thürlimann, B. (1978), "Shear strength of reinforced and prestressed concrete", *CEB Bull Inf*, **126**, 16–38.

Vecchio, F.J. and Collins, M.P. (1986), "The modified compression-field theory for reinforced concrete elements subjected to shear", *ACI Struct. J.*, **83**(2), 219–231.

Walraven, J., Belletti, B. and Esposito, R. (2013), "Shear capacity of normal, lightweight, and high-strength concrete beams according to Model Code 2010. I: Experimental results versus analytical model results", *J. Struct. Eng.*, **139**(9): 1593–1599. https://doi.org/10.1061/(ASCE)ST.1943-541X.0000742.

Wang, Q., Guo, Z. and Hoogenboom, P.C. (2005), "Experimental investigation on the shear capacity of RC dapped end beams and design recommendations", *Struct. Eng. Mech.*, **21**(2), 221-235. http://dx.doi.org/10.12989/sem.2005.21.2.221.

Yavuz, G. (2016), "Shear strength estimation of RC deep beams using the ANN and strut-and-tie approaches", *Struct. Eng. Mech.*, **57**(4), 657-680. http://dx.doi.org/10.12989/sem.2016.57.4.657.

Zhang, T., Visintin, P. and Oehlers, D.J. (2015), "Shear strength of RC beams with steel stirrups", *J Struct Eng*, **142**(2), 04015135. https://doi.org/10.1061/(ASCE)ST.1943-541X.0001404.

CC